Dynamic migration of γδ intraepithelial lymphocytes requires occludin

Karen L. Edelblum[a], Le Shen[a,b], Christopher R. Weber[a], Amanda M. Marchiando[a], Bryan S. Clay[c], Yingmin Wang[a], Immo Prinz[d], Bernard Malissen[e], Anne I. Sperling[c,1], and Jerrold R. Turner[a,f,1,2]

[a]Department of Pathology, [b]Department of Surgery, [c]Section of Pulmonary and Critical Care, Department of Medicine, and [f]Section of Gastroenterology, Department of Medicine, University of Chicago, Chicago, IL 60637; [d]Institute for Immunology, Hannover Medical School, 30625 Hannover, Germany; and [e]Centre d'Immunologie de Marseille-Luminy, Université de la Méditerranée, 13288 Marseille, France

Edited by Ronald N. Germain, National Institutes of Health, Bethesda, MD, and accepted by the Editorial Board March 16, 2012 (received for review August 9, 2011)

γδ intraepithelial lymphocytes (IELs) are located beneath or between adjacent intestinal epithelial cells and are thought to contribute to homeostasis and disease pathogenesis. Using in vivo microscopy to image jejunal mucosa of GFP γδ T-cell transgenic mice, we discovered that γδ IELs migrate actively within the intraepithelial compartment and into the lamina propria. As a result, each γδ IEL contacts multiple epithelial cells. Occludin is concentrated at sites of γδ IEL/epithelial interaction, where it forms a ring surrounding the γδ IEL. In vitro analyses showed that occludin is expressed by epithelial and γδ T cells and that occludin derived from both cell types contributes to these rings and to γδ IEL migration within epithelial monolayers. In vivo TNF administration, which results in epithelial occludin endocytosis, reduces γδ IEL migration. Further in vivo analyses demonstrated that occludin KO γδ T cells are defective in both initial accumulation and migration within the intraepithelial compartment. These data challenge the paradigm that γδ IELs are stationary in the intestinal epithelium and demonstrate that γδ IELs migrate dynamically to make extensive contacts with epithelial cells. The identification of occludin as an essential factor in γδ IEL migration provides insight into the molecular regulation of γδ IEL/epithelial interactions.

intestine | tight junction

The intestine is one of the few peripheral tissues to contain a large population of intraepithelial lymphocytes (IELs), with one IEL for every 5–10 epithelial cells. Although the majority of these IELs express the γδ T cell receptor, and epidermal γδ IELs have been studied extensively (1–4), the functions of intestinal γδ IELs remain poorly understood. Some studies have shown that γδ IELs contribute to progression of immune-mediated colitis (5–7); other data suggest that γδ IELs contribute to mucosal homeostasis (8, 9) by secreting keratinocyte growth factor (10, 11) and antimicrobial peptides (12, 13), suppressing $CD4^+$ T-cell expansion through TGF-β and IL-10 production (8, 9) and promoting barrier maintenance via poorly understood mechanisms (13–15). These observations and the small number of IELs relative to intestinal epithelial cells are difficult to reconcile with the widely held belief that γδ IELs have limited motility (1, 16).

Further understanding of γδ IEL function will require definition of the molecular structures that regulate interactions between intestinal epithelial and γδ T cells. On the basis of the location of epithelial/γδ IEL contact sites along epithelial lateral membranes, it is likely that epithelial proteins targeted to these domains, including apical junction complex components, are involved in these interactions. Attractive candidates include E-cadherin, which can bind CD103 ($\alpha_E\beta_7$ integrin) expressed by IELs (17), as well as tight junction proteins. For example, γδ IELs express several epithelial tight junction proteins, including occludin and zonula occludens-1 (ZO-1) (18), that may bind directly or indirectly to their epithelial counterparts. However, the contributions of these and other proteins to γδ IEL behavior are incompletely understood.

To determine the extent of γδ T-cell/epithelial interactions in the intestine, we used high-resolution in vivo imaging to stably visualize GFP-labeled γδ IELs in living mouse jejunum. This allows stable imaging of hundreds of cells over the course of hours while maintaining vascular and autonomic integrity. The data show that intestinal γδ T cells migrate dynamically between lamina propria and intraepithelial compartments. In the latter location, γδ T cells move along the basement membrane and also migrate into the lateral intercellular space, resulting in extensive contact with intestinal epithelia. Although both γδ IEL and epithelial expression of the tight junction protein occludin contribute to γδ IEL migration, in vitro and in vivo analyses show that γδ IEL occludin is more critical to this process. These data directly contradict the prevailing view of γδ IELs as immobile within the epithelium and demonstrate that γδ IELs provide extensive coverage of the intestinal epithelium by migrating within the intraepithelial compartment through a unique, occludin-dependent mechanism.

Results

γδ IELs Migrate Dynamically Within the Intestinal Epithelium. The small intestinal mucosa is defined by long, slender villi that arise from proliferative crypts. Sections orthogonal to this traditional longitudinal orientation allow visualization of the lumen, villous epithelium, underlying basement membrane (BM), and lamina propria (Fig. S1*A*). IELs (Fig. S1*A*, arrow) are found both along the BM and between epithelial cells in the lateral intercellular space (Fig. S1*A*, arrowhead).

To assess γδ IEL behavior within the intraepithelial compartment, GFP γδ T-cell reporter mice (TcrdEGFP) (19) were crossed with transgenic mice expressing monomeric red fluorescent protein 1 (mRFP1)-ZO-1 in the intestinal epithelium under the control of the villin promoter (20). The small intestinal mucosa of these mice was imaged in vivo by time-lapse confocal microscopy while maintaining innervation and vascular perfusion (Fig. S1*B* and Movie S1) (20). This approach allows extended high-magnification imaging of a single field, without artifacts of peristalsis, pulsatile blood flow, breathing, or other extraneous movements. These in vivo images show that within a single villus, γδ IELs migrate from the basal epithelial surface to the lateral intercellular space, approach the tight junction, and then migrate back toward the BM (Fig. 1*A* and Fig. S1*C*). This migration into

Author contributions: K.L.E., A.I.S., and J.R.T. designed research; K.L.E., L.S., C.R.W., A.M.M., B.S.C., Y.W., A.I.S., and J.R.T. performed research; I.P. and B.M. contributed new reagents/analytic tools; K.L.E., A.I.S., and J.R.T. analyzed data; and K.L.E., A.I.S., and J.R.T. wrote the paper.

The authors declare no conflict of interest.

This article is a PNAS Direct Submission. R.N.G. is a guest editor invited by the Editorial Board.

[1]A.I.S. and J.R.T. contributed equally to this work.

[2]To whom correspondence should be addressed. E-mail: jturner@bsd.uchicago.edu.

This article contains supporting information online at www.pnas.org/lookup/suppl/doi:10.1073/pnas.1112519109/-/DCSupplemental.

and out of the lateral intercellular space occurs over an average interval of 6.4 ± 0.3 min, with maximal instantaneous speed of 7.7 μm/min and an overall average speed of 3.8 ± 0.1 μm/min (Table 1). Thus, γδ IELs migrate actively within the subepithelial space, along the BM, regularly enter the lateral intercellular space, and then reverse direction along the same track to return to the subepithelial space (Movies S1 and S2). Notably, γδ IELs were never observed crossing the tight junction to enter the lumen.

Each γδ IEL transiently interacted with multiple epithelial cells (Fig. 1*A*), resulting in each epithelial cell being contacted by a γδ IEL 3.5 ± 0.2 times per hour (Fig. 1*B* and Movie S3). γδ T cells also crossed the BM to migrate between the lamina propria and intraepithelial compartment, allowing γδ IELs to survey the majority of the villous epithelium and superficial lamina propria over the course of 1 h (Fig. 1*B*). Analysis of the distance between individual γδ IELs and the lumen showed that, at any given time, 32% ± 3.3% of γδ IELs (n = 144) were located within the lateral intercellular space (dark blue) (i.e., within 15 μm of the lumen). An additional 44% ± 4.7% of γδ IELs were within the peri-BM space, 16–30 μm from the lumen (light blue), whereas only 24% ± 8.4% were more than 31 μm from the lumen (yellow).

The location of γδ IELs within the lateral intercellular space suggests that intercellular junction proteins may be involved in intraepithelial migration. If junction-associated proteins contribute to γδ IEL intraepithelial migration, one might expect a change in their distributions at sites of γδ IEL/epithelial contact. Consistent with this hypothesis, the transmembrane protein occludin was concentrated along epithelial lateral membranes, below the plane of the tight junction, and formed a continuous ring that surrounded each γδ IEL (Fig. 1*C*). Occludin expression was not detected in γδ T cells located in the lamina propria. In contrast, the cytosolic protein ZO-1 was concentrated in discrete punctae at sites of γδ IEL/epithelial contact. The localization of E-cadherin, claudin-5, and claudin-15 was not altered in the presence of a γδ IEL (Fig. S2), indicating that occludin and ZO-1 may be potential regulators of γδ IEL/epithelial interactions.

On the basis of our previous observation that the proinflammatory cytokine TNF promotes reorganization of tight junction proteins (20, 21) (Fig. S1*D*), small intestinal mucosa of TcrdEGFP mice was imaged 90 and 180 min after TNF injection (5 μg, i.p.). TNF treatment dramatically reduced γδ IEL migration and retention in the epithelium (3.3% ± 2.5%, 3.7 ± 0.6 min, respectively) (Table 1) while increasing γδ T-cell migration speed (4.3 ± 0.1 μm/min).

Taken together, these imaging studies demonstrate that γδ IELs move transiently into lateral intracellular spaces and contact multiple epithelial cells while migrating along the BM. This results in extensive coverage of the entire villous epithelium at regular intervals (Fig. 1*B*). Furthermore, the tight junction proteins occludin and ZO-1 are concentrated at sites of γδ IEL/epithelial interaction. Finally, the data show that disruption of mucosal homeostasis, with the associated occludin removal from the tight junction, is sufficient to impair γδ IEL migration into lateral intercellular spaces of the epithelial monolayer.

Epithelial and γδ IEL Occludin Form a Continuous Ring at Sites of γδ IEL/Epithelial Contact. To elucidate the mechanism by which γδ IELs migrate into the epithelium, we investigated potential mediators of γδ IEL/epithelial interactions. Several reports indicate that IELs express junction-associated proteins, including occludin, junctional adhesion molecule-A, ZO-1, β-catenin, and the E-cadherin ligand CD103 (14, 15, 18, 22). Immunostaining showed that γδ, but not αβ, IELs express ZO-1 and occludin (Fig. S3). Quantitative RT-PCR confirmed that γδ IELs transcribe message for ZO-1 and occludin and to a lesser extent claudin-4 and -7, but not claudin-1, -3, -5, or -15 (Fig. S3*C*).

To investigate the impact of occludin and ZO-1 on γδ IEL migration, we adapted an approach for time-lapse imaging of intraepithelial IEL migration ex vivo (23). γδ IELs from TcrdEGFP transgenic mice were applied to the basal aspect of a Caco-2 monolayer grown on the underside of a semipermeable filter (Fig. S4 *A* and *B*). This model recapitulated the topology and kinetics of in vivo γδ IEL behavior, with T cells migrating across the filter into the monolayer and back across the filter within several minutes (Movie S4). The number of γδ IELs within lateral intercellular spaces was maximal between 15 and 18 h after their addition to the monolayers (Fig. S4*C*), although γδ IELs were detected in lateral intercellular spaces within 3 h. Interestingly, αβ IELs migrated less efficiently than γδ IELs at all time points. It is tempting to speculate that the relatively inefficient migration of αβ IELs may be related to their lack of occludin and ZO-1 expression (Fig. S3*B*).

To determine whether apical junction proteins were redistributed at sites of γδ IEL/epithelial contact in vitro, monolayers used for migration assays were fixed and immunostained. As noted in vivo, occludin was concentrated around γδ IELs within the monolayer (Fig. 1*C* and Fig. S5 *A* and *B*), forming a continuous ring surrounding the γδ IEL surface. Similar to γδ IEL/epithelial contact sites in vivo, ZO-1 was found at discrete punctae along the periphery of the γδ IEL in epithelial monolayers (Fig. 2*B* and Fig. S5*C*). In contrast, claudin-1 and -2 were not relocalized, nor was E-cadherin redistributed at sites of γδ IEL/epithelial interaction (Fig. S5 *D*–*F*).

On the basis of our observations of occludin rings at sites of γδ IEL/epithelial interaction, we assessed the localization of the other members of the tight junction-associated MARVEL protein family, tricellulin and marvelD3 (24), at γδ IEL/epithelial contacts. MarvelD3 was absent at these sites, but tricellulin partially surrounded the γδ IEL in the lateral intercellular space, although not to the same extent as occludin (Fig. S5 *G* and *H*). Taken together, these data show that γδ IEL migration into the epithelial monolayer triggers reorganization of occludin and ZO-1 at γδ IEL/epithelial contacts without disrupting the distribution of these proteins at the epithelial tight junction.

To determine the origin of occludin within the rings, wild-type γδ IELs were applied to wild-type or occludin knockdown (KD)

Table 1. γδ IEL migration and localization in vivo

Genotype	% γδ T cells in lateral intercellular spaces	% γδ T cells in peri-BM space	Retention in epithelium (min)	Maximum track speed (μm/min)	No. of γδ IEL interactions/ epithelial cell per h
TcrdEGFP (WT)	32 ± 3.3	44 ± 4.7	6.4 ± 0.3	3.8 ± 0.1	3.5 ± 0.2
TNF (5 μg, 90 min)	3.3 ± 2.5*	40 ± 7.9*	3.7 ± 0.6*	4.3 ± 0.1*	5.9 ± 0.2*
CD103 KO	44 ± 3.5*	34 ± 0.2*	4.4 ± 0.4*	4.5 ± 0.1*	4.1 ± 0.2
WT chimera	41 ± 8.6	35 ± 9.3	n.d.	4.7 ± 0.1	4.2 ± 0.4
Occludin KO chimera	13 ± 4.1†	33 ± 4.7	n.d.	3.9 ± 0.1†	0.7 ± 0.1†

n.d., not determined.
*P < 0.01 vs. TcrdEGFP (WT).
†P < 0.01 vs. WT chimera.

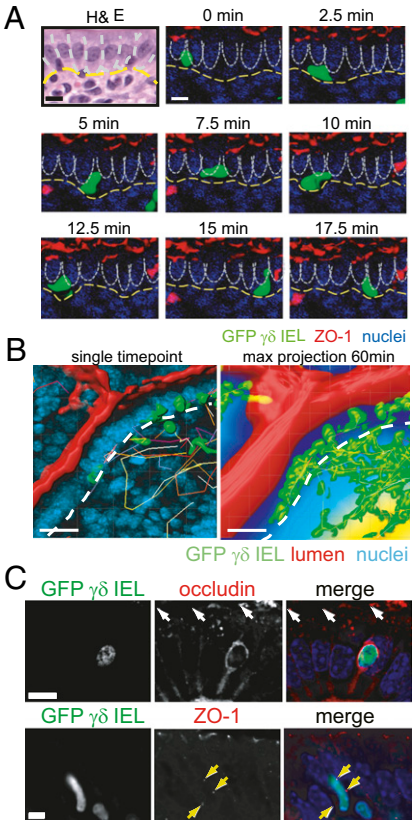

Fig. 1. γδ IELs migrate dynamically within the intestinal epithelium. (*A*) Time-lapse images of a migrating GFP γδ IEL (green) within the jejunal villous epithelium of a transgenic mouse expressing mRFP-ZO-1 (red), to label tight junctions, and injected with Hoechst dye (blue) to label epithelial nuclei. Lateral membranes of adjacent epithelial cells are indicated by dashed white lines and the BM by a dashed yellow line (Movie S3). (Scale bars, 10 μm.) (*B*) A single time point (*Left*) and 60 min maximum projection (*Right*) of γδ IEL migration. GFP γδ IEL (green), the luminal marker Alexa Fluor 633 (red), and Hoechst-labeled nuclei (blue) are shown. The BM is indicated by a dashed white line. For the maximum projection, distance from the lumen is pseudocolored; 0–15 μm, dark blue; 16–30 μm, light blue; >30 μm, yellow. The small region of green signal in the lumen is an artifact of the projection. (Scale bars, 20 μm.) (*C*) Occludin or ZO-1 (red) were immunolabeled in jejunum from GFP γδ T-cell (green) transgenic mice. Nuclei are labeled with Hoechst (blue). The epithelial tight junction is indicated by white arrows. Punctae of ZO-1 adjacent to the T cell is indicated by yellow arrows. (Scale bars, 10 μm.)

epithelial monolayers (25). Application of wild-type γδ IELs to occludin KD epithelial monolayers did not prevent formation of an occludin ring at γδ IEL/epithelial contacts (Fig. 2*B*). Because the occludin KD epithelial cells express negligible amounts of occludin (Fig. 2*B* and Fig. S5*I*), this occludin is likely expressed by γδ IELs (Fig. S3 *B* and *C*). Occludin rings also formed around occludin KO γδ IELs applied to wild-type monolayers (Fig. 2*B* and Fig. S5*J*). However, no occludin was detected at sites of γδ IEL/epithelial contact when both γδ IELs and epithelial monolayers were occludin-deficient (Fig. S5*J*). Thus, occludin produced by both γδ IELs and intestinal epithelia is recruited to sites of γδ IEL/epithelial contact.

Epithelial and γδ IEL Occludin both Contribute to in Vitro Intraepithelial γδ IEL Migration. The concentration of occludin and ZO-1 at sites of γδ IEL/epithelial contact suggests that these proteins may contribute to γδ IEL migration. To test this hypothesis, migration of wild-type or occludin KO γδ IELs into wild-type, ZO-1 KD, or occludin KD Caco-2 monolayers (Fig. S5*I*) was assessed (26). Wild-type γδ IEL migration into occludin-deficient monolayers was reduced by 58% ± 7% relative to wild-type γδ IEL migration into wild-type monolayers. This was specific to occludin; migration of wild-type γδ IELs into ZO-1 KD monolayers was similar to migration into wild-type monolayers. Thus, epithelial occludin is an important mediator of γδ IEL migration (Fig. 2*C*).

To determine the role of γδ IEL-derived occludin in γδ IEL/epithelial interactions, γδ IELs isolated from occludin KO mice (27–29) were applied to wild-type Caco-2 monolayers. Occludin KO γδ IELs exhibited a 73% ± 5% reduction in migration compared with wild-type γδ IELs (Fig. 2*C*). No further reduction in γδ IEL migration occurred when occludin KO γδ IELs were applied to occludin KD monolayers (Fig. 2*C*). Thus, although epithelial occludin does facilitate γδ IEL migration, γδ IEL occludin seems to play a greater role.

Although the effect of occludin knockdown was remarkable, a small amount of γδ IEL migration persisted. We hypothesized that this might be attributable to E-cadherin–CD103 interactions; however, migration of CD103 KO γδ IELs was comparable to that of wild-type γδ IELs, suggesting that CD103 does not contribute to γδ T-cell intraepithelial migration in vitro (Fig. 2*D*).

To determine whether the in vitro data reflected in vivo biology, γδ IEL migration was assessed in CD103 KO mice (Table 1). Although the extent of migration into lateral intercellular spaces was not reduced, γδ IELs lacking CD103 were retained in the epithelium for less time (4.4 ± 0.4 min) and exhibited an increased migratory speed (4.5 ± 0.1 μm/min) relative to wild-type γδ IELs. Thus, rather than mediate γδ IEL migration into the epithelium, CD103–E-cadherin interactions may serve to stabilize γδ IEL/epithelial interactions.

Occludin Expressed by γδ T Cells Is Essential for Efficient Recruitment to and Migration Within the Intestinal Epithelium in Vivo. Our in vitro studies provide a potential mechanism by which γδ IELs interact with epithelial cells; however, the reductionist ex vivo system we have developed does not recapitulate in vivo tissue complexity. Thus, to assess the contribution of γδ IEL occludin to in vivo migration, mixed bone marrow chimeras were generated by transplanting 80% γδ T cell–deficient bone marrow supplemented with either 20% wild-type GFP γδ T-cell or occludin KO GFP γδ T-cell bone marrow into lethally irradiated hosts. The number of GFP γδ T cells was assessed in the spleen, small intestinal lamina propria, and small intestinal intraepithelial compartments 8 wk after transplant. The number of GFP γδ T cells in the spleen and lamina propria was similar in both wild-type and occludin KO γδ T-cell mixed bone marrow chimeras, suggesting that occludin deficiency did not compromise engraftment or trafficking to the intestine (Fig. 3*A*). In contrast, accumulation of occludin KO GFP γδ T cells within the intraepithelial compartment was markedly reduced relative to wild-type GFP γδ T cells. This defect in occludin KO γδ T-cell accumulation within the intraepithelial compartment was corrected by 16 wk after engraftment, consistent with our observation that intraepithelial γδ IEL numbers are comparable in adult wild-type and occludin KO mice. This suggests that occludin KO γδ T cells fill the intestinal intraepithelial compartment inefficiently but are eventually able to establish a quantitatively normal population at this site. Interestingly, and possibly related to this delay, analysis of IELs showed reduced GFP and γδ T-cell receptor expression in occludin KO, but not wild-type, γδ T-cell chimeras at 8 wk after engraftment (Fig. S6*A*).

Engrafted wild-type γδ IELs migrated apically to reside in lateral intercellular spaces, similar to γδ IELs in TcrdEGFP transgenic mice (Fig. 3*B* and Fig. S1*C*). In contrast, occludin KO γδ IELs within the epithelial compartment remained in the subepithelial space, between the basal epithelial surface and BM (Fig. 3*B*). At any given time, 41% ± 8.6% of engrafted wild-type γδ IELs (n = 1134) were present within the first 15 μm of the lumen, the region corresponding to lateral intercellular spaces,

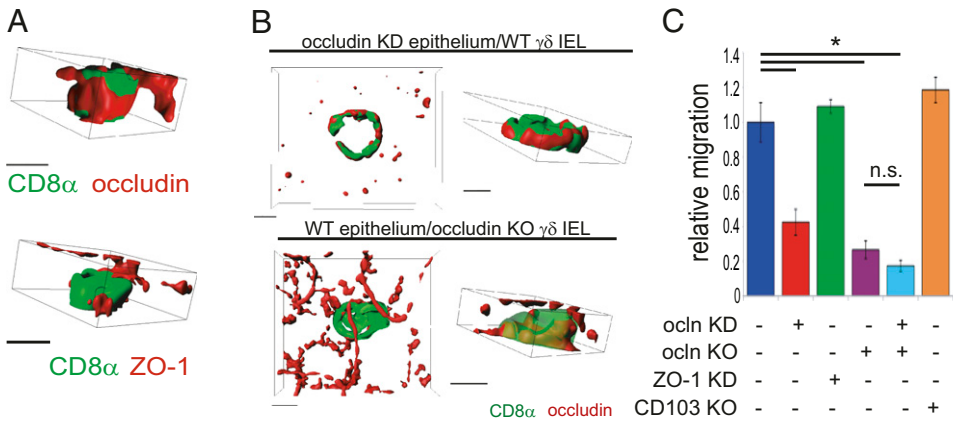

Fig. 2. Occludin forms rings at sites of γδ IEL/epithelial contact and promotes γδ IEL migration into epithelial monolayers. (*A*) 3D reconstructions, viewed from the lateral membrane, of isolated γδ IELs (CD8α, green) that have migrated into cultured epithelial monolayers. Occludin or ZO-1 is shown in red. (Scale bars, 5 μm.) (*B*) 3D reconstructions of wild-type γδ IELs (CD8α, green) within occludin KD epithelium or occludin KO γδ IELs within wild-type epithelium. Occludin is shown in red. (Scale bars, 5 μm.) (*C*) Morphometric analysis of wild-type, occludin, or CD103 KO γδ IEL migration into wild-type, occludin-, or ZO-1–deficient epithelium ($n = 3$). $P < 0.001$.

compared to only 13% ± 4.1% of occludin KO γδ IELs (n = 2,042) (Fig. 3*C* and Fig. S6*B*). Occludin KO γδ IELs were predominantly found within the peri-BM lamina propria, at distances between 16 and 30 μm from the lumen (33% ± 4.7%). Thus, although the proportions of wild-type and occludin KO γδ IELs above the BM are similar (Fig. S6*C*), occludin KO γδ IELs migrate a shorter distance into the lateral intercellular space compared with wild-type γδ IELs (Fig. S6*D*). The elongation of an IEL between adjacent epithelial cells does not account for this difference, because both wild-type and occludin KO γδ IELs occupy a similar fraction of the lateral intercellular space (Fig. S6*E*).

In addition to differences in localization, KO γδ IELs migrated at rates significantly lower than wild-type γδ IELs (Fig. 3 *D* and *E* and Movies S5 and S6). As a result, each epithelial cell was contacted by an occludin KO γδ IEL only 0.7 ± 0.1 times per hour (n = 74), which represents a greater than 80% reduction relative to the 4.2 ± 0.4 times per hour (n = 33) that a wild-type γδ IEL contacted an epithelial cell. These data show that migration of occludin KO γδ T cells within the intraepithelial compartment is defective and that this defect results in reduced coverage of the epithelial monolayer relative to wild-type γδ IELs. GFP γδ IEL migration was similarly impaired in occludin KO mice, which is consistent with our in vitro data, suggesting that the absence of γδ IEL occludin causes a defect that is quantitatively similar to combined loss of epithelial and γδ T-cell occludin (Fig. 2*C*). Thus, in addition to regulating epithelial barrier properties (20, 24, 25, 30), occludin is essential to γδ IEL migration as well as their extensive interactions with the intestinal epithelium.

Last, to determine whether occludin is required for γδ T-cell migration in tissues other than the intestinal mucosa, spleens of TcrdEGFP mice were imaged (2, 3). The average migration speed of splenic γδ T cells was reduced relative to IELs. Whereas

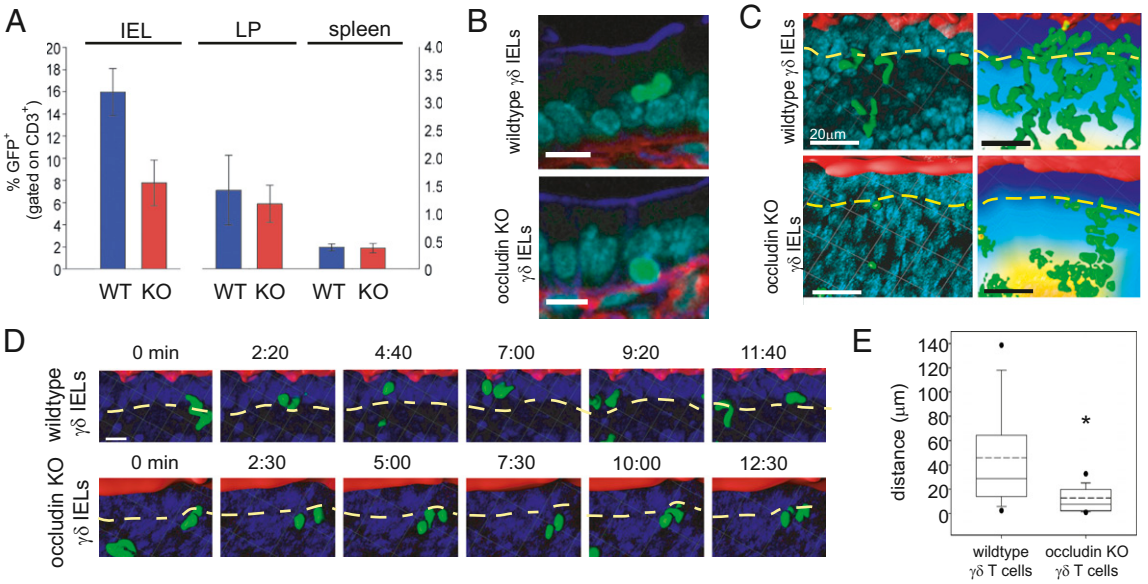

Fig. 3. Occludin is required for γδ IEL migration in vivo. Mixed bone marrow chimeras were generated to express wild-type or occludin KO GFP γδ T cells in T-cell–deficient hosts. (*A*) Flow cytometric analysis of $CD3^+$ T cells expressing GFP in small intestinal IELs, lamina propria lymphocytes (LP), or splenocytes isolated from wild-type or occludin KO γδ IEL chimeras, as indicated. (*B*) Jejunum of wild-type or occludin KO GFP γδ chimeras labeled to detect GFP (green), F-actin (blue), laminin (red), and nuclei (cyan). (Scale bars, 20 μm.) (*C*) A single time point (*Left*) and 60-min maximum projection (*Right*) of GFP γδ IEL migration in wild-type and occludin KO γδ IEL chimeras. γδ IEL (green), ZO-1 and intestinal lumen (red), nuclei (blue). The BM is indicated by a dashed yellow line. Distance from the lumen is pseudocolored as described in Fig. 1*B*. (Scale bars, 20 μm.) (*D*) Time-lapse images taken from Movies S5 and S6 show wild-type or occludin KO γδ IEL (green) migration over ≈20 min. Intestinal lumen (red) and nuclei (blue) are shown. The BM is indicated by a dashed yellow line. (Scale bar, 10 μm.) (*E*) Distance of γδ splenocyte tracks in GFP γδ wild-type or GFP γδ occludin KO mice. $P < 0.001$.

wild-type γδ splenocytes migrated slightly slower than occludin KO γδ splenocytes (Fig. S6*F*), the distance covered by occludin KO splenocytes was markedly reduced compared with wild-type (Fig. 3*E*). Similar studies were attempted in the skin, but very few dermal γδ T cells were detected in TcrdEGFP mice (Fig. S6*G*), and no migration of these cells was observed during video microscopy. Nevertheless, the altered migration within the spleen suggests that occludin contributes to γδ T cell migration in organs other than the intestine. However, in the spleen we anticipate that γδ T cell occludin interacts with dendritic or endothelial cell-expressed occludin.

Discussion

Although trafficking of γδ T cells between extraintestinal sites and the intestinal intraepithelial compartment has been studied extensively (1, 16, 31–33), intraepithelial migration has not been well characterized (16). Consequently, IELs are generally perceived as being "sessile" (1) cells with "very limited basal motility" (16). Thus, it remains unclear how γδ T cells interact with the epithelium and mucosal microenvironment to impact intestinal biology. Our data demonstrate that γδ IELs migrate rapidly and extensively within the confined space of the intraepithelial compartment to efficiently survey large areas of villous epithelium. This provides a potential explanation for the proposed roles of γδ IELs in global mucosal homeostasis, despite their limited abundance relative to epithelial cells. We have also identified the epithelial tight junction protein occludin as an essential mediator of this migration and, remarkably, have found that both γδ IEL and epithelial occludin expression are necessary for in vitro and in vivo intraepithelial γδ IEL migration. Furthermore, TNF-mediated epithelial barrier dysfunction prevents γδ IEL migration into lateral intercellular spaces and increases the speed of those γδ IELs scanning the epithelial monolayer along the BM.

Recent work demonstrated that γδ T-cell migration within axillary lymph nodes is rapid; however, the examination of intraepithelial γδ IEL migration could not be completely resolved from artifacts caused by residual peristaltic movement (16). In contrast, the approach used here stabilized an externalized loop of jejunum and allowed the villi to be imaged for up to 5 h with little extraneous movement. The limited movement of luminal markers, fluorescent-tagged epithelial proteins, and epithelial nuclei over time confirmed this stability and eliminated peristalsis, breathing, and pulsatile blood flow as confounding artifacts. Furthermore, time-lapse images (Figs. 1*B* and 3*D*) demonstrate that γδ IELs move along independent and divergent paths rather than back and forth along a single trajectory, as might be expected as a result of artifactual peristaltic movement. This ability to image hundreds of cells over hours allowed a large sample size and a quantitative appraisal of IEL migration. These data suggest that the speed of cell migration is not a sufficient measure of overall migratory capacity but that cell migration rate should be considered relative to the environment. Thus, this imaging approach provides the ability to visualize γδ IEL migration in intestinal villi, which will be useful in understanding the role of γδ IEL/epithelial interactions in intestinal physiology and disease.

Occludin KO mice do not display an overt intestinal or immune phenotype (29), and, despite extensive study, the role of occludin in regulation of epithelial barrier function remains controversial (20, 24, 25, 30, 34–37). However, dominant-negative mutant occludin expression within cultured epithelial monolayers did reduce in vitro neutrophil transmigration, raising the possibility that occludin may contribute to interactions between epithelial and other immune cells (38). Occludin expression has also been reported in dendritic cells (22, 39), where it has been suggested that interactions between dendritic and epithelial cell occludin may allow dendritic processes to penetrate the tight junction and reach into the lumen without disrupting the barrier (39). Although this hypothesis has not been tested experimentally, such a function in dendritic cells is likely different from that in γδ IELs, because our data demonstrate that, in contrast to dendritic cells, γδ IELs do not cross the epithelial tight junction.

Notably, intestinal γδ IELs seem to freely cross the BM to enter the intraepithelial compartment from the lamina propria. This contrasts sharply with reports of CXCR6-GFP+ γδ T cell migration in the skin (2, 3). It is possible that this difference reflects the distinct architectures of the epidermal stratified squamous epithelium and the intestinal simple columnar epithelium.

Both γδ IEL and epithelial occludin contribute to the rings observed at sites of γδ IEL/epithelial contact (Figs. 1*C* and 2 *A* and *B* and Fig. S5). Although epithelial occludin is concentrated at the tight junction, it does exchange between the tight junction and lateral membrane domains (40), suggesting that this lateral membrane pool is the source of epithelial occludin at sites of IEL contact. However, epithelial occludin is still localized at these sites in the absence of γδ IEL occludin (Fig. 2*B*), indicating that binding to γδ IEL occludin cannot be the trigger that recruits epithelial occludin. Nevertheless, direct interactions between γδ IEL and epithelial occludin may still be an important step in sensing γδ IEL movement into the lateral intercellular space. This may explain why migration is impaired in response to TNF, which induces occludin internalization (Fig. S1*D*) (20, 41). Although not defined, the contribution of occludin–occludin interactions may be to induce epithelial cells to modify their shape to make space for the migrating γδ IEL or promote additional intercellular interactions through IEL membrane proteins such as CD103, epithelial cell adhesion molecule (42), or junctional adhesion molecule ligand (43). Alternatively, transient occludin accumulation along the epithelial basolateral surface may function as a cue for γδ IEL recruitment into a targeted site within the epithelial monolayer.

γδ IELs are involved in the regulation of the mucosal microenvironment in response to intestinal disease, including inflammatory bowel disease (44), celiac disease, graft-vs.-host disease (45), and parasite infection (14, 15). However, the precise role of γδ IELs remains controversial. Our data demonstrating the ability of γδ IELs to migrate and contact multiple epithelial cells over a short time provide a potential mechanism by which γδ IELs, which are greatly outnumbered by epithelial cells, can impact the entire epithelium. This migration can also be considered a form of surveillance that regulates intracellular signaling in both by γδ IELs and epithelial cells to prevent epithelial injury and infection (12–15). The acceleration of γδ T-cell migration within the peri-BM and lamina propria compartments after TNF treatment may therefore represent a form of innate immune activation (Table 1). It will, therefore, be important to define the contributions of γδ IEL/epithelial interactions to mucosal homeostasis and changes in γδ IEL migration during disease.

In summary, we used rapid, high-resolution in vivo imaging of stable jejunal mucosa to demonstrate that γδ IEL migration within the subepithelial and lateral intercellular space is highly dynamic and occurs via an occludin-dependent mechanism. These data challenge the widely held view that intestinal IELs are sessile and indicate that γδ IEL migration may explain how these cells regulate intestinal function. These results and the techniques developed for in vitro and in vivo analysis of γδ IEL migration and localization both provide insight and create opportunities to advance the understanding of γδ IEL interactions with the intestinal epithelium and function in homeostasis and disease.

Materials and Methods

Animals and Live Imaging. Mice aged 8–12 wk maintained on a C57BL/6 background were used for all experiments. Wild-type and Tcrd KO mice were obtained from The Jackson Laboratories. Occludin KO mice were provided by M. Neville (University of Colorado, Denver, CO) and backcrossed onto a C57BL/6 background for at least 10 generations (29). TcrdH2BeGFP (TcrdEGFP) mice (19) were crossed to occludin KO or villin-

mRFP1-ZO-1 transgenic mice (20). Mice were injected i.p. with 5 μg of TNF (Peprotech) and imaged 90–180 min after injection. All studies were conducted in an Association for Assessment and Accreditation of Laboratory Animal Care (AAALAC)-accredited facility under protocols approved by the University of Chicago Institutional Animal Care and Use Committee.

Imaging was performed as described previously (20); details are provided in *SI Materials and Methods*. Postacquisition analysis was performed using Imaris (Bitplane, version 7.1.0), MetaMorph (Molecular Devices, version 7), and ImageJ. Using Imaris, a surface was created for the EGFP channel to render GFP γδ T cells, which were tracked using autoregressive motion with a maximum distance of 15 μm and a maximum gap size of 3. Individual tracks were checked and corrected manually when necessary. Only tracks with a duration >2 min were included.

Bone Marrow Chimeras. Mice were lethally irradiated with 11 Gy γ-irradiation. Twenty-four hours after irradiation, mice were reconstituted by i.v. injection of 4×10^6 Tcrd KO bone marrow cells and 1×10^6 of either wild-type TcrdEGFP or TcrdEGFP; occludin KO bone marrow cells. Imaging was performed 8 wk after engraftment.

In Vitro Studies. IEL migration assays into Caco-2_{BBe} monolayers (24, 26) were performed placing flow cytometry-sorted IELs in the upper chamber of the Transwell and fixing the filters at various time points. Stable cell lines expressing pSUPER vectors containing occludin (36) or ZO-1 (26) targeting sequence resulted in the suppression of 90% of target protein expression in Caco-2_{BBe} cells (46). Further information can be found in *SI Materials and Methods*.

Statistical Analyses. All data are presented as ± SEM and represent three independent experiments. *P* values of direct comparisons between two independent samples were determined by a two-tailed Student *t* test and were considered to be significant if $P \leq 0.05$. Alternatively, ANOVA was used and the overall effect was tested at $P = 0.05$ to control the type I error rate. Fisher's exact test was used to compare proportions between two independent variables, and the Mann-Whitney test was used compare groups that do not have a normal distribution.

ACKNOWLEDGMENTS. We thank V. Bindokas and the University of Chicago Integrated Light Microscopy Core Facility for confocal microscopy and image analysis support, the University of Chicago Flow Cytometry Facility, and A.-C. France for statistical analysis. This work was supported by National Institutes of Health Grants T32HL007237, F32DK084859, and K01DK093627 (to K.L.E.), K08DK088953 (to C.R.W.), Environmental Protection Agency (EPA) RD-83406701-0 and R01AI067697 (to A.I.S.), and R01DK61931, R01DK68271, P01DK67887, and S10RR025643 (to J.R.T.); University of Chicago Digestive Disease Research Core Center Grant P30DK42086; University of Chicago Institute for Translational Medicine Grant UL1RR024999; University of Chicago Comprehensive Cancer Center Grant P30CA14599; Department of Defense Grant W81XWH-09-1-0341 (to J.R.T.); and the Crohn's and Colitis Foundation of America (L.S.).

1. Swamy M, Jamora C, Havran W, Hayday A (2010) Epithelial decision makers: In search of the 'epimmunome'. *Nat Immunol* 11:656–665.
2. Sumaria N, et al. (2011) Cutaneous immunosurveillance by self-renewing dermal gammadelta T cells. *J Exp Med* 208:505–518.
3. Gray EE, Suzuki K, Cyster JG (2011) Cutting edge: Identification of a motile IL-17-producing gammadelta T cell population in the dermis. *J Immunol* 186:6091–6095.
4. Chodaczek G, Papanna V, Zal MA, Zal T (2012) Body-barrier surveillance by epidermal γδ TCRs. *Nat Immunol* 13:272–282.
5. Nanno M, et al. (2008) Exacerbating role of gammadelta T cells in chronic colitis of T-cell receptor alpha mutant mice. *Gastroenterology* 134:481–490.
6. Park SG, et al. (2010) T regulatory cells maintain intestinal homeostasis by suppressing γδ T cells. *Immunity* 33:791–803.
7. Do JS, et al. (2010) Cutting edge: Spontaneous development of IL-17-producing gamma delta T cells in the thymus occurs via a TGF-beta 1-dependent mechanism. *J Immunol* 184:1675–1679.
8. Tsuchiya T, et al. (2003) Role of gamma delta T cells in the inflammatory response of experimental colitis mice. *J Immunol* 171:5507–5513.
9. Inagaki-Ohara K, et al. (2004) Mucosal T cells bearing TCRgammadelta play a protective role in intestinal inflammation. *J Immunol* 173:1390–1398.
10. Boismenu R, Havran WL (1994) Modulation of epithelial cell growth by intraepithelial gamma delta T cells. *Science* 266:1253–1255.
11. Chen Y, Chou K, Fuchs E, Havran WL, Boismenu R (2002) Protection of the intestinal mucosa by intraepithelial gamma delta T cells. *Proc Natl Acad Sci USA* 99:14338–14343.
12. Ismail AS, Behrendt CL, Hooper LV (2009) Reciprocal interactions between commensal bacteria and gamma delta intraepithelial lymphocytes during mucosal injury. *J Immunol* 182:3047–3054.
13. Ismail AS, et al. (2011) Gammadelta intraepithelial lymphocytes are essential mediators of host-microbial homeostasis at the intestinal mucosal surface. *Proc Natl Acad Sci USA* 108:8743–8748.
14. Dalton JE, et al. (2006) Intraepithelial gammadelta+ lymphocytes maintain the integrity of intestinal epithelial tight junctions in response to infection. *Gastroenterology* 131:818–829.
15. Inagaki-Ohara K, et al. (2006) Intestinal intraepithelial lymphocytes sustain the epithelial barrier function against *Eimeria vermiformis* infection. *Infect Immun* 74:5292–5301.
16. Chennupati V, et al. (2010) Intra- and intercompartmental movement of gammadelta T cells: Intestinal intraepithelial and peripheral gammadelta T cells represent exclusive nonoverlapping populations with distinct migration characteristics. *J Immunol* 185:5160–5168.
17. Higgins JM, et al. (1998) Direct and regulated interaction of integrin alphaEbeta7 with E-cadherin. *J Cell Biol* 140:197–210.
18. Inagaki-Ohara K, Sawaguchi A, Suganuma T, Matsuzaki G, Nawa Y (2005) Intraepithelial lymphocytes express junctional molecules in murine small intestine. *Biochem Biophys Res Commun* 331:977–983.
19. Prinz I, et al. (2006) Visualization of the earliest steps of gammadelta T cell development in the adult thymus. *Nat Immunol* 7:995–1003.
20. Marchiando AM, et al. (2010) Caveolin-1-dependent occludin endocytosis is required for TNF-induced tight junction regulation in vivo. *J Cell Biol* 189:111–126.
21. Clayburgh DR, et al. (2005) Epithelial myosin light chain kinase-dependent barrier dysfunction mediates T cell activation-induced diarrhea in vivo. *J Clin Invest* 115:2702–2715.
22. Alexander JS, et al. (1998) Activated T-lymphocytes express occludin, a component of tight junctions. *Inflammation* 22:573–582.
23. Shaw SK, et al. (1998) Migration of intestinal intraepithelial lymphocytes into a polarized epithelial monolayer. *Am J Physiol* 275:G584–G591.
24. Raleigh DR, et al. (2010) Tight junction-associated MARVEL proteins marveld3, tricellulin, and occludin have distinct but overlapping functions. *Mol Biol Cell* 21:1200–1213.
25. Raleigh DR, et al. (2011) Occludin S408 phosphorylation regulates tight junction protein interactions and barrier function. *J Cell Biol* 193:565–582.
26. Yu D, et al. (2010) MLCK-dependent exchange and actin binding region-dependent anchoring of ZO-1 regulate tight junction barrier function. *Proc Natl Acad Sci USA* 107:8237–8241.
27. Schulzke JD, et al. (2005) Epithelial transport and barrier function in occludin-deficient mice. *Biochim Biophys Acta* 1669:34–42.
28. Saitou M, et al. (1998) Occludin-deficient embryonic stem cells can differentiate into polarized epithelial cells bearing tight junctions. *J Cell Biol* 141:397–408.
29. Saitou M, et al. (2000) Complex phenotype of mice lacking occludin, a component of tight junction strands. *Mol Biol Cell* 11:4131–4142.
30. Van Itallie CM, Fanning AS, Holmes J, Anderson JM (2010) Occludin is required for cytokine-induced regulation of tight junction barriers. *J Cell Sci* 123:2844–2852.
31. Pauls K, et al. (2001) Role of integrin alphaE(CD103)beta7 for tissue-specific epidermal localization of CD8+ T lymphocytes. *J Invest Dermatol* 117:569–575.
32. Schön MP, et al. (1999) Mucosal T lymphocyte numbers are selectively reduced in integrin alpha E (CD103)-deficient mice. *J Immunol* 162:6641–6649.
33. Cepek KL, Parker CM, Madara JL, Brenner MB (1993) Integrin alpha E beta 7 mediates adhesion of T lymphocytes to epithelial cells. *J Immunol* 150:3459–3470.
34. Musch MW, Walsh-Reitz MM, Chang EB (2006) Roles of ZO-1, occludin, and actin in oxidant-induced barrier disruption. *Am J Physiol Gastrointest Liver Physiol* 290:G222–G231.
35. Yu AS, et al. (2005) Knockdown of occludin expression leads to diverse phenotypic alterations in epithelial cells. *Am J Physiol Cell Physiol* 288:C1231–C1241.
36. Seth A, Sheth P, Elias BC, Rao R (2007) Protein phosphatases 2A and 1 interact with occludin and negatively regulate the assembly of tight junctions in the CACO-2 cell monolayer. *J Biol Chem* 282:11487–11498.
37. Murakami T, Felinski EA, Antonetti DA (2009) Occludin phosphorylation and ubiquitination regulate tight junction trafficking and vascular endothelial growth factor-induced permeability. *J Biol Chem* 284:21036–21046.
38. Huber D, Balda MS, Matter K (2000) Occludin modulates transepithelial migration of neutrophils. *J Biol Chem* 275:5773–5778.
39. Rescigno M, et al. (2001) Dendritic cells express tight junction proteins and penetrate gut epithelial monolayers to sample bacteria. *Nat Immunol* 2:361–367.
40. Shen L, Weber CR, Turner JR (2008) The tight junction protein complex undergoes rapid and continuous molecular remodeling at steady state. *J Cell Biol* 181:683–695.
41. Shen L, et al. (2006) Myosin light chain phosphorylation regulates barrier function by remodeling tight junction structure. *J Cell Sci* 119:2095–2106.
42. Nochi T, et al. (2004) Biological role of Ep-CAM in the physical interaction between epithelial cells and lymphocytes in intestinal epithelium. *Clin Immunol* 113:326–339.
43. Witherden DA, et al. (2010) The junctional adhesion molecule JAML is a costimulatory receptor for epithelial gammadelta T cell activation. *Science* 329:1205–1210.
44. McVay LD, et al. (1997) Changes in human mucosal gamma delta T cell repertoire and function associated with the disease process in inflammatory bowel disease. *Mol Med* 3:183–203.
45. Maeda Y, et al. (2005) Critical role of host gammadelta T cells in experimental acute graft-versus-host disease. *Blood* 106:749–755.
46. Turner JR, et al. (1997) Physiological regulation of epithelial tight junctions is associated with myosin light-chain phosphorylation. *Am J Physiol* 273:C1378–C1385.

Supporting Information

Edelblum et al. 10.1073/pnas.1112519109

SI Materials and Methods

Live Imaging Experiments. Mice were anesthetized, injected i.v. with Hoechst 33342 dye, and a jejunal loop was exposed and opened along the antimesenteric border, as previously described (1). The mucosa was placed against a coverslip bottom of a 35-mm Petri dish containing 0.15 mL either HBSS or 1 μM Alexa Fluor 633 in HBSS, and the body of the mouse was laid over the opened jejunal segment. Alternatively, the spleen was externalized through a small incision and held in place by a single suture of the surrounding connective tissue to the skin. Dermis was imaged as previously described (2). A multiphoton confocal inverted microscope (SP5; Leica) with a 40× 0.8 N.A. water immersion objective was used. EGFP was imaged using an Argon laser with a spectral emission of 491–580 nm, monomeric red fluorescent protein (mRFP)1 was imaged using a laser (DPSS 561) with a spectral emission of 589–727, and Alexa Fluor 633 was imaged with a spectral emission of 640–769 nm. Pinholes of 160, 190, and 150 μm were used for these three channels, respectively. Hoechst dye was imaged using a multiphoton laser and a pinhole of 600 μm. Scanning was performed at 8,000 Hz, and all images were acquired using LAS-AF software (Leica, version 6.3.1). Images were acquired by taking 15-μm Z-stacks at 1.5-μm spacing. The total time of acquisition for a single Z-stack ranged between 50 and 70 s. Distance from γδ T cells to the apical surface, either mRFP–zonula occludens-1 (ZO-1) or free Alexa 633, was measured in Imaris (Bitplane) by creating a separate surface for the apical marker and performing a distance transformation to attain the distance of a γδ T cell from the apical surface at any given time.

Immunofluorescence and Image Analysis. Mouse jejunum was fixed in 2% paraformaldehyde for 2 h, washed with 50 mM NH_4Cl, and cryoprotected in 30% sucrose (wt/vol) at 4 °C overnight. Tissue was snap-frozen in Optimal Cutting Temperature (OCT) medium and stored at −80 °C. Frozen sections were immunostained as previously described (3) and examined using a DMLB epifluorescence microscope equipped with an 88000 filter set (Chroma Technology), 20× 0.7 N.A. dry or a 63× PLAN APO 1.32 N.A. oil immersion objective, Retiga EXi camera and Metamorph 7 acquisition software. Z-stacks were deconvolved with Autodeblur for 10 iterations.

Intraepithelial lymphocytes (IELs) migrating into Caco-2_{BBe} monolayers grown on Transwells were fixed with ice-cold methanol or 1% (wt/vol) paraformaldehyde. Transwells were allowed to air dry, permeabilized with 0.1% (wt/vol) saponin, and blocked with 5% (wt/vol) BSA. After immunostaining, filters were mounted and visualized as described above. 3D reconstructions were generated using Imaris. Migration was assessed by manually counting the number of IELs within the focal plane of the epithelial monolayer.

IEL Lamina Propria Lymphocyte (LPL) Isolation and Flow Cytometry. Mice were killed, small intestines excised, and Peyer's patches removed. The small intestine was opened longitudinally, rinsed in Ca^{2+}- and Mg^{2+}-free HBSS (Sigma-Aldrich), and incubated in HBSS with 5% (wt/vol) FBS (Cellgro) and 2 mM EDTA for 1 h at 37 °C. Supernatants were applied to packed glass wool columns, and IELs were pelleted and purified on discontinuous 20/45/70% (wt/vol) Percoll gradients (GE Healthcare Life Sciences). Surface receptor staining was performed after blocking with anti-Fc receptor antibody CD16/32 (eBioscience), using PerCP-anti-CD3, phycoerythrin (PE)- or APC-anti-γδT-cell receptor, and FITC- or PE-anti-βTCR antibodies (eBioscience). IELs were sorted to 98% purity on the basis of GFP or TCR expression using a FACSAria IIu (BD Pharmingen). Flow cytometric analysis was performed on a FACS Canto (BD Pharmingen) and data analyzed with FlowJo software (TreeStar).

Cell Culture and Generation of Stable Knockdown Cell Lines. Caco-2_{BBe} cells were cultured as previously described (4, 5) and plated on inverted 3.0-μm collagen-coated polycarbonate Transwells (Corning). Experiments were performed 10 d after confluence. Flow cytometry-sorted IELs were place in the upper chamber of the Transwell, and filters were collected and fixed at various time points. pSUPER vectors containing occludin (6) or ZO-1 (5) targeting sequence were used to stably transfect Caco-2_{BBe} cells (7). This suppressed >90% of target protein expression. Control cell lines were generated by stable transfection of pSUPER vectors expressing related, but ineffective, shRNA sequences.

RNA Isolation, RT, and Quantitative Real-Time PCR. Small intestinal IELs were expanded in vitro as previously described (8) and sorted according to GFP expression. After lysis in TRIzol (Invitrogen), RNA was extracted with chloroform, precipitated, and purified using an RNeasy mini kit (Qiagen). cDNA was synthesized with reverse transcriptase (Invitrogen), and mRNA was quantified by SYBR green real-time PCR (Bio-Rad) using validated primers (9).

1. Marchiando AM, et al. (2010) Caveolin-1-dependent occludin endocytosis is required for TNF-induced tight junction regulation in vivo. *J Cell Biol* 189:111–126.
2. Gray EE, Suzuki K, Cyster JG (2011) Cutting edge: Identification of a motile IL-17-producing gammadelta T cell population in the dermis. *J Immunol* 186:6091–6095.
3. Marchiando AM, et al. (2010) Caveolin-1-dependent occludin endocytosis is required for TNF-induced tight junction regulation in vivo. *J Cell Biol* 189:111–126.
4. Raleigh DR, et al. (2010) Tight junction-associated MARVEL proteins marveld3, tricellulin, and occludin have distinct but overlapping functions. *Mol Biol Cell* 21:1200–1213.
5. Yu D, et al. (2010) MLCK-dependent exchange and actin binding region-dependent anchoring of ZO-1 regulate tight junction barrier function. *Proc Natl Acad Sci USA* 107: 8237–8241.
6. Yu AS, et al. (2005) Knockdown of occludin expression leads to diverse phenotypic alterations in epithelial cells. *Am J Physiol Cell Physiol* 288:C1231–C1241.
7. Turner JR, et al. (1997) Physiological regulation of epithelial tight junctions is associated with myosin light-chain phosphorylation. *Am J Physiol* 273:C1378–C1385.
8. Sperling AI, Linsley PS, Barrett TA, Bluestone JA (1993) CD28-mediated costimulation is necessary for the activation of T cell receptor-gamma delta+ T lymphocytes. *J Immunol* 151:6043–6050.
9. Holmes JL, Van Itallie CM, Rasmussen JE, Anderson JM (2006) Claudin profiling in the mouse during postnatal intestinal development and along the gastrointestinal tract reveals complex expression patterns. *Gene Expr Patterns* 6:581–588.

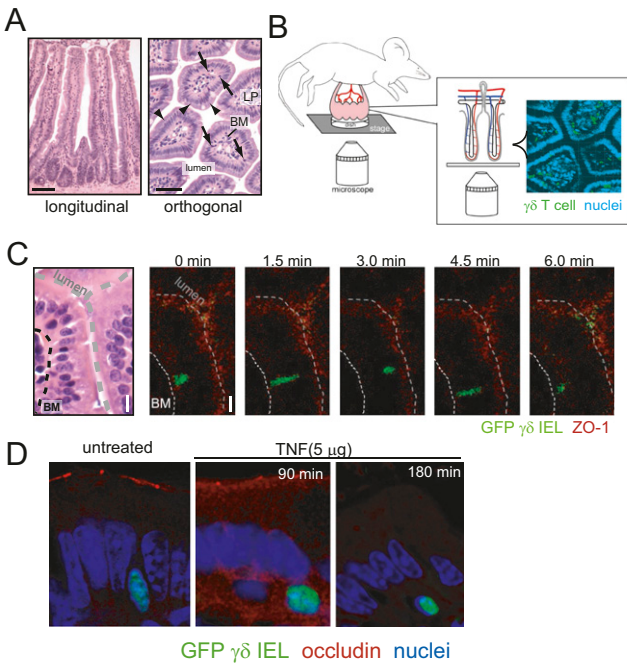

Fig. S1. γδ IELs move into and along the intestinal epithelium. (*A*) An H&E stain of fixed jejunum shows a longitudinal section through the crypt-villus axis (*Left*) or an orthogonal section through several villi (*Right*). IELs (arrows) are located along the basement membrane (BM) and in lateral intercellular spaces between epithelial cells (arrowheads). (Scale bars, 50 μm.) (*B*) A cartoon illustrating live imaging of γδ IELs in an orthogonal plane of jejunal villi of TcrdEGFP mice (Movie S1). Nuclei (blue), γδ T cells (green). (*C*) Time-lapse images of a GFP γδ IEL (green) migrating into the lateral intercellular space. mRFP-ZO-1 (red), BM (white line), lumen (gray line). H&E image is shown for orientation. (Scale bars, 10 μm.) (*D*) Occludin (red) localization in untreated and TNF-treated (5 μg, 90 and 180 min after injection) TcrdEGFP mice. Nuclei are shown in blue and γδ IELs in green.

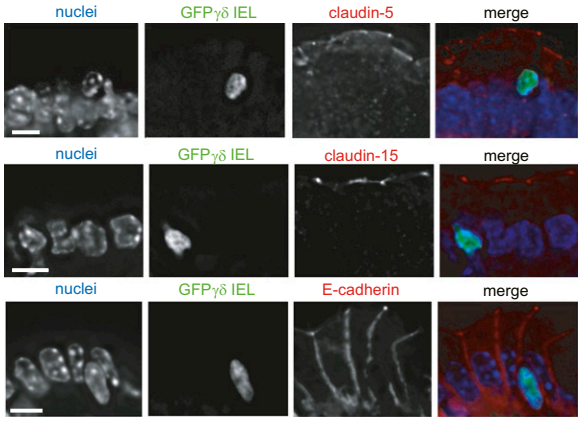

Fig. S2. Distributions of claudin-5, claudin-15, and E-cadherin are not changed at sites of γδ IEL/epithelial contact. Jejunum from GFP γδ T-cell (green) transgenic mice was harvested and immunostained for junction proteins, as indicated (red). Nuclei are shown in blue. (Scale bars, 10 μm.)

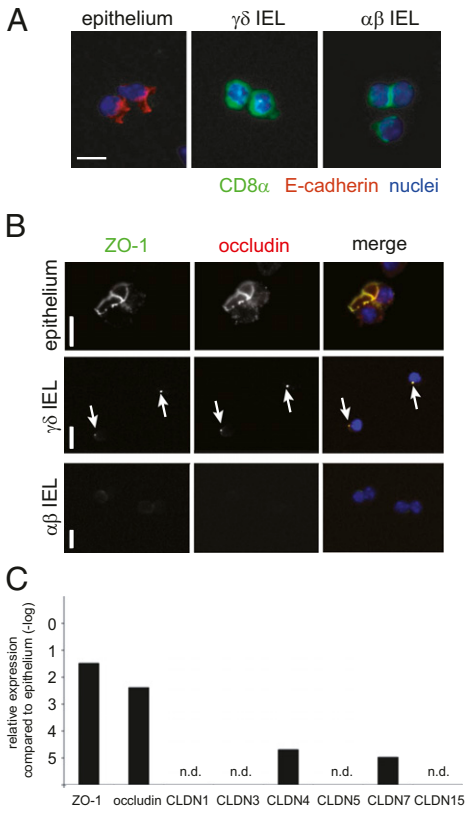

Fig. S3. γδ IELs express occludin and ZO-1. (*A*) Epithelial cells, γδ IELs, and αβ IELs were fixed and stained for CD8α (green), E-cadherin (red), or nuclei (blue). (*B*) Tight junction protein expression was assessed by immunofluorescence for ZO-1 (green) and occludin (red). (*C*) Real-time PCR for tight junction proteins was performed on epithelial cells or γδ IELs. mRNA expression was normalized to GAPDH. Data for γδ IELs are expressed relative to comparable normalized expression in epithelial cells (-log).

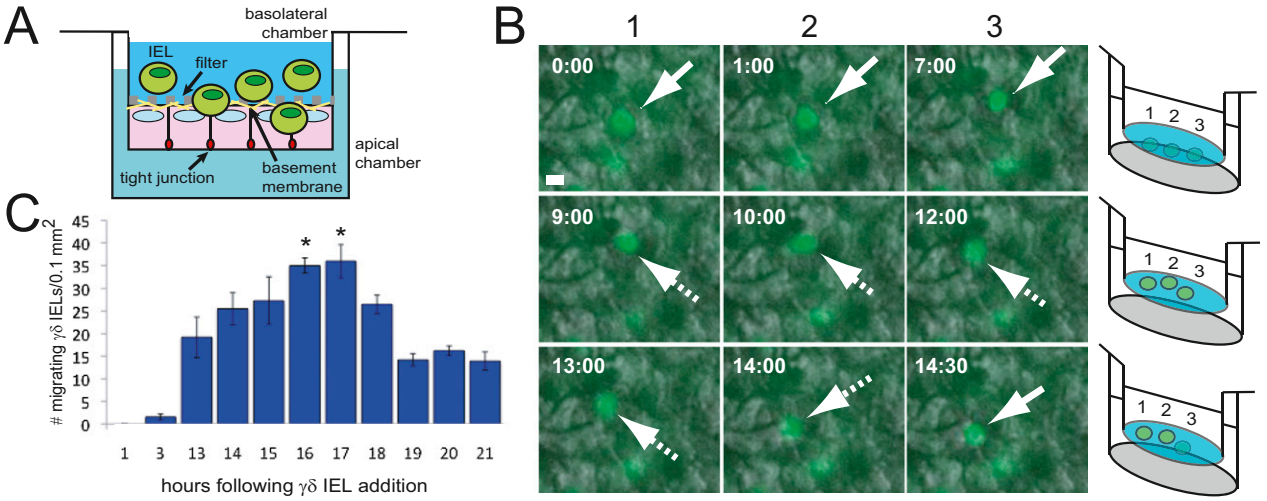

Fig. S4. γδ IELs migrate dynamically into intestinal epithelial monolayers. (*A*) Diagram of in vitro migration assay. (*B*) Time-lapse images taken from video microscopy of GFP γδ IELs migrating into a monolayer as viewed from the apical surface (Movie S4). Solid arrows indicate a γδ IEL located within the monolayer, dashed arrows indicate a γδ IEL under the Transwell filter. On the right, cartoons indicate the position of each IEL in relation to the filter. The numbers correspond to the images in the panel. (Scale bar, 5 μm.) (*C*) Morphometric analysis of γδ IELs migrating through the Transwell filter into the epithelial monolayer over the time course indicated ($n = 3$), $P < 0.01$.

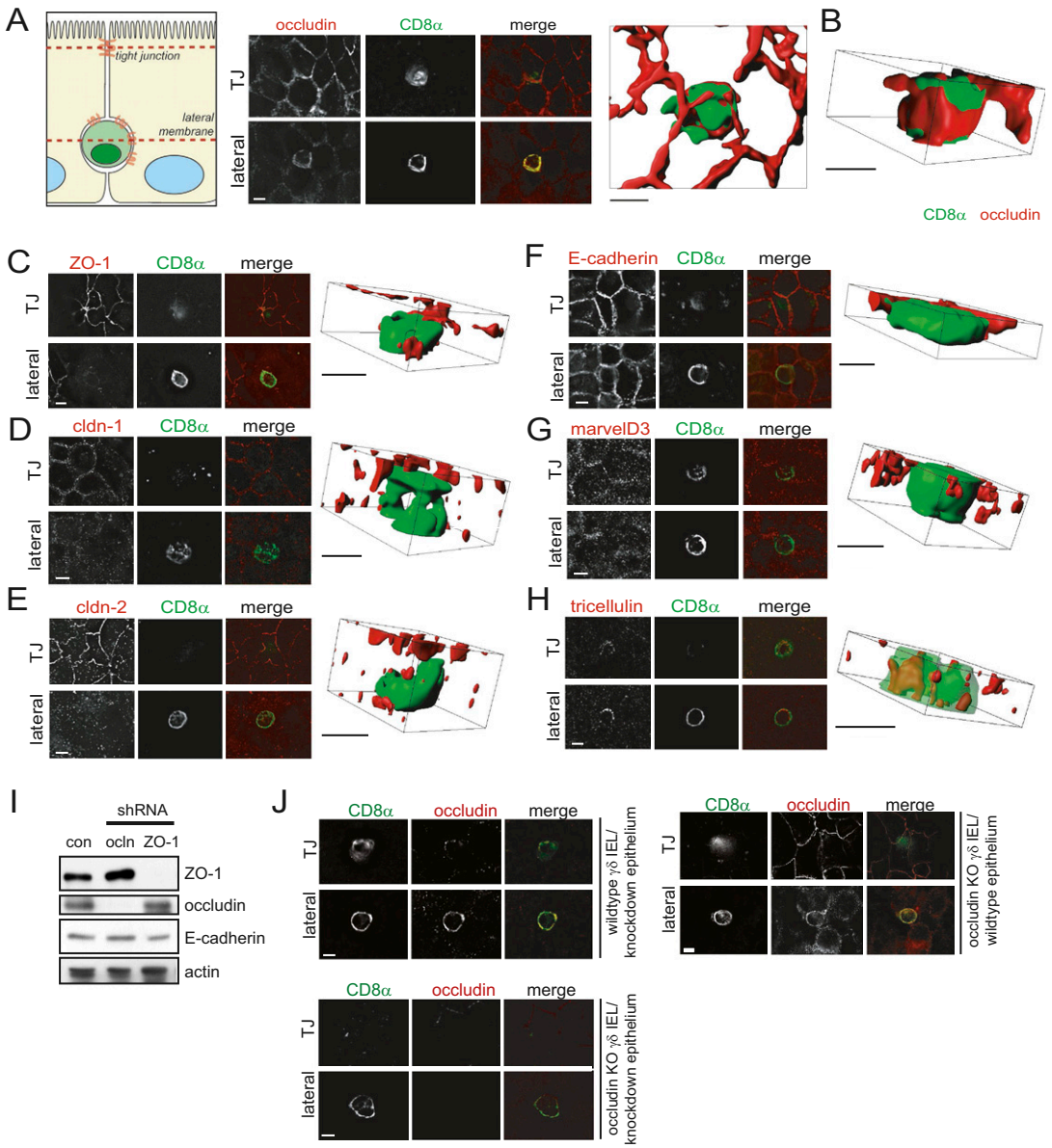

Fig. S5. Epithelial- and γδ IEL-derived occludin contribute to occludin rings observed at sites of γδ IEL/epithelial contact. Cultured epithelial monolayers into which containing γδ IELs (CD8α, green) had migrated in vitro were fixed and immunostained for tight junction proteins (red) (*A* and *B*) occludin, (*C*) ZO-1, (*D*) claudin-1, (*E*) claudin-2, (*F*) E-cadherin, (*G*) tricellulin, and (*H*) marvelD3. Z-sections at the level of the tight junction (TJ) and from the lateral membrane are shown (*A*). XY plane sections are shown from the apical surface or a lateral point within the monolayer, as indicated. 3D reconstructions are shown at the right of each set of XY plane images. (Scale bars, 5 μm.) (*I*) Western blot analysis of ZO-1, occluding, and E-cadherin in Caco-2_{BBe} cell clones with stable knockdown of occludin or ZO-1. Actin serves as a loading control. (*J*) Immunostaining of a wild-type γδ IEL within occludin knockdown epithelium or an occludin KO γδ IEL within wild-type or occludin knockdown epithelium. CD8α (green) and occludin (red) are shown. (Scale bars, 5 μm.)

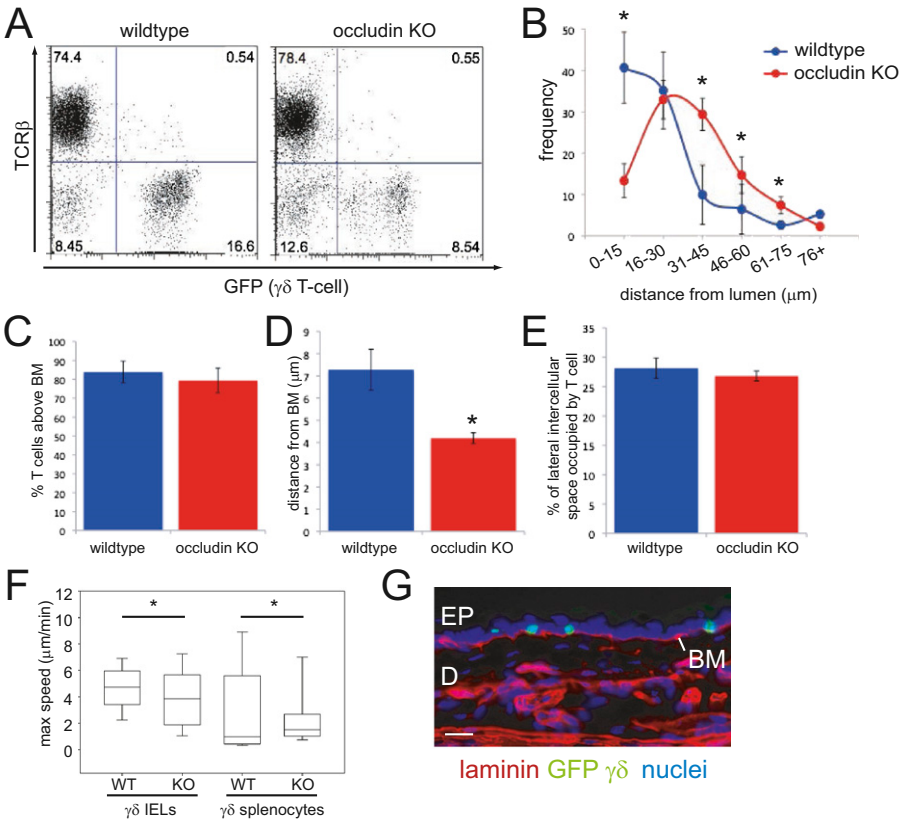

Fig. S6. Occludin KO γδ IELs inefficiently repopulate and migrate into the intraepithelial compartment. (*A*) GFP and TCRβ expression in small intestinal IELs isolated from wild-type or occludin KO γδ IEL chimeras. (*B*) Distance of wild-type and occludin KO γδ IELs from the intestinal lumen (μm), $P < 0.001$. (*C*) Fraction of γδ T cells above the BM in wild-type and occludin KO chimeras. (*D*) Distance (μm) of wild-type or occludin KO γδ IELs from the BM. $P < 0.01$. (*E*) Percentage of the epithelial lateral intercellular space occupied by a γδ IEL. (*F*) Maximum speed of wild-type and occludin KO γδ IELs or γδ splenocytes. $P < 0.001$. (*G*) Skin from the ear of a TcrdEGFP mouse was stained with laminin (red). Nuclei (blue) and γδ T cells (green) are shown. EP, epithelium; D, dermis. (Scale bar,30 μm.)

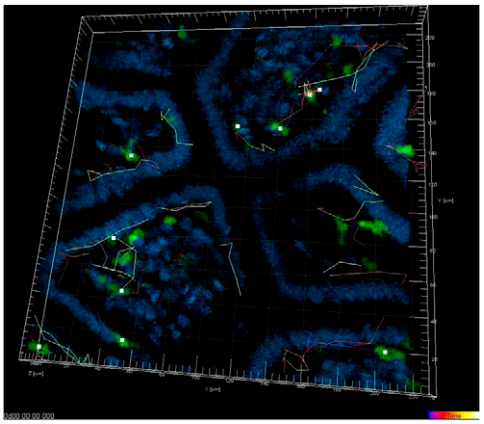

Movie S1. Time-lapse live imaging showing GFP γδ T cells migrating in jejunal villi. GFP γδ T cells (green) migrate dynamically along the BM and into epithelial lateral intercellular spaces (nuclei, blue).

Movie S1

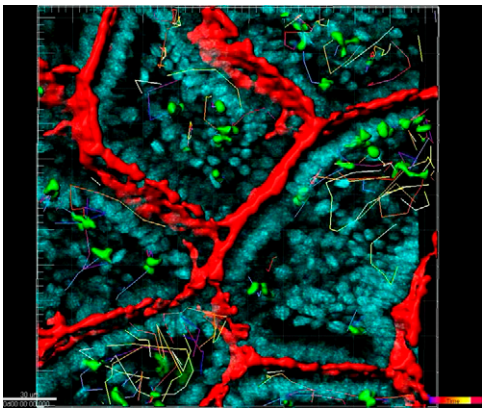

Movie S2. GFP γδ T cells interact with multiple epithelial cells. GFP γδ T cells (green), nuclei (blue), Alexa 633 (red) is used as a luminal marker.

Movie S2

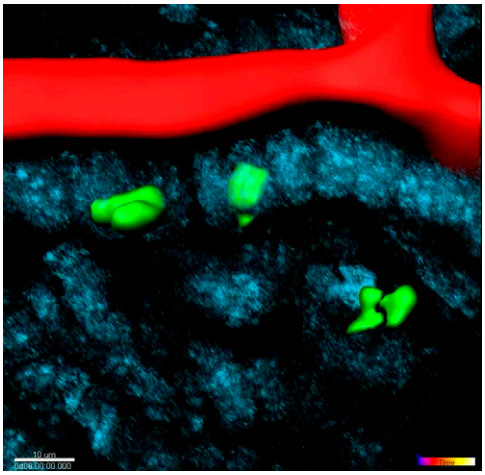

Movie S3. GFP γδ IELs migrate dynamically within the intraepithelial compartment. GFP γδ T cells (green), nuclei (blue), Alexa 633 (red) is used as a luminal marker.

Movie S3

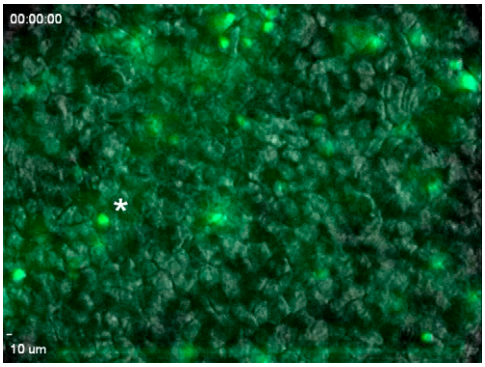

Movie S4. GFP γδ T cells migrate in and out of a Caco-2 monolayer. GFP γδ T cells (green), epithelium (phase), a white asterisk marks the γδ IEL within the epithelial monolayer.

Movie S4

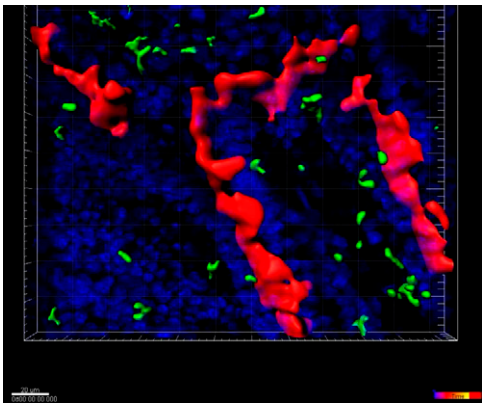

Movie S5. GFP γδ T cells in a wild-type γδ T-cell mixed bone marrow chimera migrate efficiently within the intestinal epithelium. GFP γδ T cells (green), nuclei (blue), mRFP-ZO-1 (red) marks the apical surface of the epithelium.

Movie S5

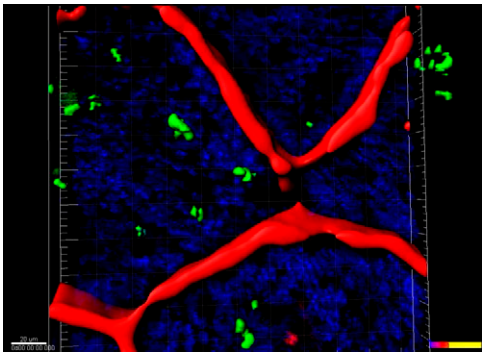

Movie S6. GFP occludin KO γδ T cells do not migrate efficiently into lateral intercellular spaces. GFP γδ T cells (green), nuclei (blue), Alexa 633 (red) is used as a luminal marker.

Movie S6